UNIVERSITY OF CALIFORNIA SAN DIEGO

Cancer Aneuploidy and T cell Dysfunction

A Thesis submitted in partial satisfaction of the requirements
for the degree Master of Science

in

Biology

by

Daniel Xu

Committee in charge:

Professor Maurizio Zanetti, Chair
Professor Cornelis Murre, Co-Chair
Professor Li-Fan Lu

2024

The Thesis of Daniel Xu is approved, and it is acceptable in quality and form for publication on microfilm and electronically.

University of California San Diego

2024

DEDICATION

To my family, who always stood by me and supported me on this journey even when the journey was uncertain.

TABLE OF CONTENTS

THESIS APPROVAL PAGE iii

DEDICATION iv

TABLE OF CONTENTS v

LIST OF FIGURES vi

LIST OF TABLES vii

LIST OF ABBREVIATIONS viii

ACKNOWLEDGEMENTS ix

VITA xi

ABSTRACT OF THE THESIS xii

INTRODUCTION 1

Chapter 1 CANCER ANEUPLOIDY DOES NOT INCREASE INDUCTION OF UPR 5

Acknowledgements 7

Chapter 2 T CELL FUNCTION IS DIMINISHED BY ANEUPLOID CM 8

Acknowledgements 10

Chapter 3 INDUCTION OF UPR ACTIVATES T CELLS 11

Acknowledgements 17

Chapter 4 EFFECT OF ANUEPLOID CM ON T CELL METABOLISM 18

Acknowledgements: 21

Chapter 5 DISCUSSION 22

MATERIALS AND METHODS 26

REFERENCES 32

LIST OF FIGURES

Figure 1: Cancer aneuploidy does not cause increased induction of UPR. 6

Figure 2: UPR is diminished in CD3 T cells activated in the presence of aneuploid CM..... 9

Figure 3: Induction of ER stress and UPR activates T cells 12

Figure 4: Induction of UPR enhances T cell activation 15

Figure 5: Agonism of the IRE1 pathway is unable to restore T cell function 16

Figure 6: Aneuploid CM reduces EZH2 expression in dysfunctional T cells 20

Figure 7: The supplementation of IXA4 to Aneuploid CM does not restore T cell function 21

LIST OF TABLES

Table 1: Reagents and Resources Table 26

Table 2: Reagents and Resources Continued 27

LIST OF ABBREVIATIONS

ATF4	Activating Transcription Factor 4
ATF6	Activating Transcription Factor 6
B16	B16.F10
CM	Conditioned Medium
DMEM	Dulbecco's Modified Eagle Medium
ER	Endoplasmic Reticulum
eIF2α	Eukaryotic Initiation Factor 2 alpha
GzmB	Granzyme Beta
IRE1	Inositol-requiring Enzyme Type 1
IFN-γ	Interferon-Gamma
PERK	Protein kinase RNA-like Endoplasmic Reticulum Kinase
p-eIF2α	Phosphorylated Eukaryotic Initiation Factor 2 alpha
RIDD	Regulated IRE1-dependent decay
Sk3	SKOV3
TCR	T cell receptor
TERS	Transmissible Endoplasmic Reticulum Stress
TIL	Tumor Infiltrating Lymphocyte
UPR	Unfolded Protein Response
XBP1	X box binding Protein 1
XBP1s	X box binding Protein 1 spliced

ACKNOWLEDGEMENTS

I would like to acknowledge Professor Maurizio Zanetti for their support as the chair of my committee and for serving as my Principle Investigator. Without his guidance and expertise this thesis would not have been able to be completed. I would also like to acknowledge Magalie Dosset for her mentoring and for teaching me a multitude of laboratory techniques and protocols that I did not know before this program. Finally I would like to acknowledge Gonzalo Almanza, his expertise and advice proved invaluable for trouble shooting experimental procedures and for acquiring new reagents.

Chapter 1 contains unpublished material coauthored with Magalie Dosset, Gonzalo Almanza, Maurizio Zanetti, Su Xian, and Hannah Carter. B16 and D5 cells in Figure 1's experiments were maintained in culture and prepared for Western Blot by Magalie Dosset, PhD. Flow cytometer machine operation for flow cytometry samples was done by Dennis Young of the Moores Cancer Flow Cytometry Core. The thesis author was the primary author of this chapter.

Chapter 2 contains unpublished material coauthored with Magalie Dosset, Gonzalo Almanza, Maurizio Zanetti, Su Xian and Hannah Carter. Flow cytometer machine operation for flow cytometry samples were run by Dennis Young of the Moores Cancer Flow Cytometry Core. Figures displaying experiments with T cells treated by B16 and D5 CM partially consist of experimental data generated by Magalie Dosset, PhD. The final presented figure is a combination of Magalie Dosset's data with my experimental data. The thesis author was the primary author of this chapter.

Chapter 3 contains unpublished material coauthored with Magalie Dosset, Gonzalo Almanza, Maurizio Zanetti, Su Xian, and Hannah Carter. The thesis author was the primary author of this chapter.

Chapter 4 contains unpublished material coauthored with Magalie Dosset, Gonzalo Almanza, Maurizio Zanetti, Su Xian, and Hannah Carter. Magalie Dosset performed the ELISA assay shown in figure 6e while I assisted with the cell treatment. The thesis author was the primary author of this chapter.

VITA

2022 Bachelor of Science in Molecular and Cell Biology, University of California San Diego

2024 Master of Science in Biology, University of California San Diego

ABSTRACT OF THE THESIS

Cancer Aneuploidy and T cell Dysfunction

by

Daniel Xu

Master of Science in Biology

University of California San Diego, 2024

Professor Maurizio Zanetti, Chair
Professor Cornelis Murre, Co-Chair

Aneuploidy, aberrant chromosome numbers, is a chromosome alteration that is associated with poor prognosis and outcome in cancer. However, the exact role aneuploidy plays in cancer progression and local immune cell regulation are a matter of debate. Here we investigate the hypothesis that aneuploidy in cancer cells triggers an ER stress that will be transmitted to T cell, ultimately driving their dysfunction. We found that the conditioned medium (CM) of aneuploid

murine B16.F10 and human SKOV3 cancer cells caused diminished Interferon-gamma (IFNG) and Granzyme B (GzmB) expression in T cells activated by anti-CD3/CD28 stimulation. However, the induction of aneuploidy in cancer cells did not result in UPR elevated enough to enable the transmission of UPR phenotype in T cells. T cells with diminished cytokine expression in response to aneuploid CM did not have an increase in UPR gene expression and the addition of UPR inhibitors could not restore IFNG or Granzyme expression. In fact, the induction of UPR, both through chemical means and transmissible ER stress factors, enhanced the function and activation of T cells rather than impairing their function. Finally, accumulating evidence indicates that glucose-restriction can contribute to the loss of T cell effector function by repressing EZH2, a subunit of Polycomb Repressive Complex 2 (PRC2). T cells made dysfunctional by aneuploid CM had significantly lower EZH2 expression which positively correlated with IFNG. However, addition of glucose to reactivate EZH2-mediate glucose metabolism only partially restored IFNG production in T cells. A provisional conclusion is that aneuploidy in cancer cells can cause T cell dysfunction in a cell-nonautonomous manner, but the mechanism behind it does not seem to depend on ER stress and glucose deprivation only provides a partial explanation. Further investigation is still needed to fully understand the molecular mechanism by which aneuploid CM impairs T cell immunity.

INTRODUCTION

Aneuploidy, defined as aberrant numbers of chromosomes, is one of the oldest known chromosomal alterations observed in cancer cells (Boveri et. al., 2008). It is part of a wider family of genetic abnormalities known as somatic copy-number alterations (SCNA) that are frequently observed in cancer cells (Beroukhim et. al., 2010). It has been observed in 90% of solid tumors and 50% of blood cancers and is associated with cancer progression and poor prognosis (Beroukhim et. al., 2010). Recently, tumor aneuploidy has been associated with markers of immune evasion, suggesting that it negatively regulates immune surveillance and by doing so confers a selective advantage to cancer cells (Davoli et. al., 2017; Xian et al 2021). Recent published work by our lab also indicates that the supernatant of aneuploid cancer cells can impair T cell function, suggesting that this immunosuppressive effect is ascribed to cell non-autonomous processes (Xian et. al., 2021). However, the molecular mechanisms by which aneuploid cancer cells drive T cell dysfunction were not explored.

Because of chromosome aberrations, aneuploid cells are subject to profound physiological changes and stressors. It has been observed that aneuploid eukaryotic cells have higher protein dosage and are particularly sensitive to disruptions in protein synthesis and folding pathways (Torres et. al., 2007). Therefore, aneuploid cancer cells are also likely subject to proteotoxic stress and rely on endoplasmic reticulum (ER) stress response as a compensatory mechanism. A growing body of evidence suggests that the ER stress response play an important role in cancer pathology and tumorigenesis, in particular through the unfolded protein response (UPR) (Chen et. al., 2020).

The mammalian UPR is a conserved network of signal transduction pathways triggered in response to proteotoxic stress (Schröder et. al., 2005). Elements of the UPR can intersect with other stress response pathways which can be triggered for instance by metabolic changes or autophagy; therefore the UPR is considered part of a broader ensemble of stress responses known as the Integrated Stress Response (ISR) (Walter and Ron, 2011). Through both transcriptional and non-transcriptional regulation, the UPR will attempt to restore proteostasis or, in the case of chronic proteotoxic stress and damage, it will trigger apoptosis (Schröder et. al., 2005). The UPR is mediated by three primary sensors: IRE1, PERK, and ATF6, each with their own signaling pathways which are in turn all regulated by a single master regulator, GRP78, which keeps them in an inactive state until it dissociates from the sensor complexes to bind misfolded proteins (Schröder et. al., 2005, Ron and Walter, 2011).

Inositol-requiring Enzyme Type 1(IRE1), is a serine threonine kinase that splices a 26 nucleotide from the X box binding protein 1 (XBP1). Spliced XBP1, often referred to as XBP1s, acts as a transcription factor for UPR genes (Yoshida et. al., 2001). IRE1 also targets ER-localized mRNA through a process known as regulated IRE1-dependent decay (RIDD) (Holien et. al., 2006). This activity increases with intensity of ER stress and can induce apoptosis by degrading anti-apoptotic mRNAs, allowing for a graded adaptive response to ER stress that becomes an apoptotic one under sufficiently high sustained ER stress (Holien et. al., 2009).

The protein kinase RNA-like endoplasmic reticulum kinase (PERK) phosphorylates eif2α in response to unfolded proteins, generating a phosphorylated eIF2α (p-eIF2α), which inhibits most protein translation except for UPR related proteins and activates specific transcription factors (Liu et. al., 2003). One particular transcription factor activated by PERK that is vital to the UPR is activating transcription factor 4 (ATF4), which activates UPR genes to restore

proteostasis. However, under intense stress ATF4 also promotes the activation of C/EBP binding protein (CHOP), which in sufficient quantity induces apoptosis (Morishima et. al., 2011). eIF2α can be phosphorylated by multiple molecules and overlaps in stress response pathways outside of the UPR, and is considered a key element of the ISR (Ryzmski et. al., 2007).

Activating Transcription Factor 6 (ATF6) is an ER bound membrane that migrates to the Golgi for cleavage after GRP78 dissociates from the luminal domain (Shen et. al., 2002). After cleavage by site 1 and then site 2 protease, the ATF6 cytosolic domain is revealed and it enters the nucleus where it activates UPR genes, including XBP1 and later CHOP (Yoshida et. al., 2001).

The uncontrolled growth and replication inherent to cancer significantly taxes the protein synthesis and folding capacity of cancer cells, particularly for cancers known be highly secretory (Obeng et. al., 2006). The genetic instability and high mutational burden imposed by cancers such as melanoma and lung cancers can also directly degrade the folding capacity of proteins (Piwocka et. al., 2006). In addition, the tumor microenvironment often imposes hypoxia and nutrient restriction that can fuel induction of ER stress response (Koumenis et. al., 2006). As a result, it is unsurprising that cancer cells are frequently under significant ER stress and must lean on the UPR to maintain homeostasis and growth (Koumenis, 2006, Piwocka et al., 2006, Obeng et. al., 2006). While the potential selective advantages conferred by cell-autonomous effects of UPR have been well documented, previous research has documented a cell non-autonomous phenomenon where cancer cells subjected to induced ER stress transmit in turn an elevated ER stress profile to surrounding cells via their secretome (Mahadevan et. al., 2011, Mahadevan et. al., 2012). This “transmissible ER stress” (TERS) confers ER stress in neighboring immune cells

and is known to shift macrophages and dendritic cells towards immunosuppressive phenotypes (Mahadevan et. al., 2011, Mahadevan et. al., 2012).

Because aneuploidy has been documented to subject eukaryotic cells to proteotoxic stress, it was initially hypothesized that aneuploidy induced a transmissible ER stress profile to aneuploidy cells which transmitted elevated ER stress and subsequent dysfunction to T cells (Zanetti, 2017). To test this hypothesis, we interrogated the cell-nonautonomous effects on T cells of two aneuploid cancer cell models: the quasi-diploid ovarian cancer cell SKOV3 treated by Reversine (SKOV3 Rv) and a clonal B16.F10 murine melanoma cell line derived by cell-cell fusion with mouse embryonic fibroblasts (D5) (Searles et al., 2018). While aneuploid cancer cells can confer dysfunction to activated T cells in a cell-non-autonomous manner, both aneuploidy cancer cells and effected T cells do not possess elevated UPR. Instead, dysfunctional T cells show diminished UPR induction and their dysfunction is aggravated by inhibition of the UPR. Furthermore, we found that aneuploid tumor cells can cause a glucose deprivation in the microenvironment that causes T cell dysfunction, however this only partially explains the observed alterations of T cell function. Altogether this suggests there are additional mechanistic links between aneuploid tumor cells and T cell dysfunction.

Chapter 1 CANCER ANEUPLOIDY DOES NOT INCREASE INDUCTION OF UPR.

To uncover if the induction of aneuploidy induces ER stress and UPR, we used two experimental aneuploidy models: the human quasi-diploid SKOV3 ovarian cancer cells treated with Reversine, referred to as SKOV3 Rv, and D5 cells, a polyploid hybrid clone derived from the murine B16.F10 melanoma cell line. SKOV3 cells were treated for 2 days with Reversine, a mitotic spindle inhibitor known to induce aneuploidy (Santaguida et. al., 2015, 2017), before being cultured in reversine free medium for 3 days. D5 cells are stably hyperploid (Searles et. al., 2018). To verify induction of ploidy, DNA content analysis of SKOV3 Rv and D5 cells were compared with control SKOV3 and B16 cells (Figure 1a). As expected, SKOV3 Rv and D5 cells had higher DNA content, and therefore increased ploidy, than control SKOV3 and B16 cells (Figure 1a). It is worth noting that B16 parental cells are not naturally diploid, and have instead an altered ploidy. However, D5 cells have significantly higher ploidy than B16 cells, thus D5 cells still provide a useful model to assess the effects of increased ploidy.

To examine if the induction of aneuploidy in cancer cells resulted in the activation of ER stress, RT-PCR was performed to analyze mRNA expression of XBP1s (Figure 1d, 1e). Compared to their parental counterpart, aneuploid SKOV3 tumor cells did not show increased XBP1s induction, in fact, XBP1 splicing tended to be reduced, (Figure 1c, 1e). Examination of protein expression of IRE1, PERK and phosphorylated eIF2α (p-eIF2α) by Western Blot showed a decrease of both IRE1 and p-eIF2α, confirming the reduced activation of the UPR in aneuploid SKOV3 cells (Figure 1c). Similar observations were made for the murine D5 melanoma model (Fig 1b, 1d). Collectively, this data suggests that the induction of aneuploidy in cancer cells does not increase the UPR and, therefore, does not favor the induction of a transmissible ER stress profile.

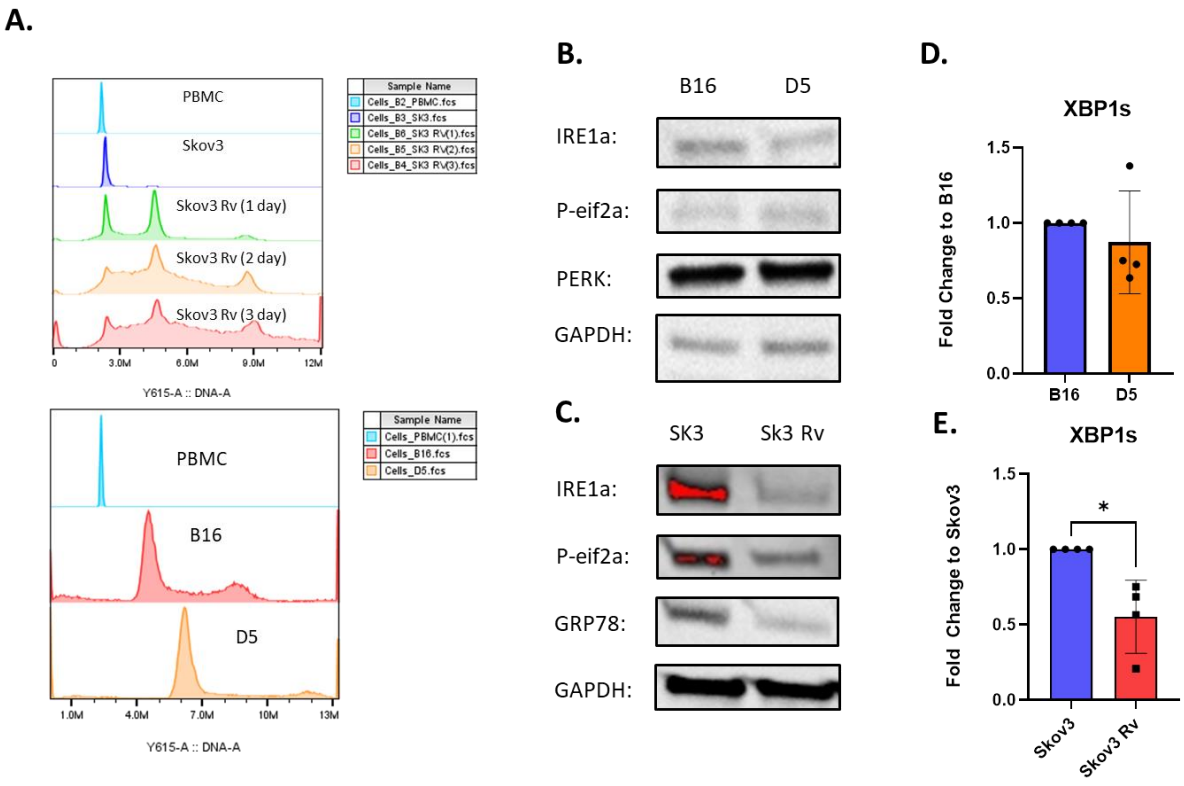

Figure 1: **Cancer aneuploidy does not cause increased induction of UPR**.

(A) Comparison of DNA content in Aneuploid SKOV3 Rv, D5 cells and control SKOV3, B16 cells by propidium iodide staining. Fluorescent intensity measured by Flow Cytometry. (B-C) Western Blot analysis of IRE1 and PERK pathway in control B16 and aneuploid D5 cells (B) or SKOV3 and SKOV3 Rv cells (C). (D) Normalized mRNA expression of XBP1s (E) Normalized mRNA expression of XBP1s in control SKOV3 and aneuploid SKOV3 Rv cells. mRNA expression is normalized to diploid control SKOV3 cells. Beta-Actin was used as an endogenous control for RT-PCR. Dots on bar graph represent triplicate experiments expressed as mean ± SD. Error bars represent mean ± 1 SD. All P values were calculated using Wilcoxon matched-pairs signed rank test. * $p \leq 0.05$, ** $p \leq 0.01$, *** $p \leq 0.001$, **** $p \leq 0.0001$.

Acknowledgements

Chapter 1 contains unpublished material coauthored with Magalie Dosset, Gonzalo Almanza, Maurizio Zanetti, Su Xian, and Hannah Carter. B16 and D5 cells in Figure 1's experiments were maintained in culture and prepared for Western Blot by Magalie Dosset, PhD. Flow cytometer machine operation for flow cytometry samples was done by Dennis Young of the Moores Cancer Flow Cytometry Core. The thesis author was the primary author of this chapter.

Chapter 2 T CELL FUNCTION IS DIMINISHED BY ANEUPLOID CM

To investigate the cell-nonautonomous effects of aneuploid cancer cells on T cells, $CD3^+$ T cells isolated from human donor blood PBMCs were activated with anti-CD3/anti-CD28 antibodies in the presence of CM of aneuploid tumor cells (Rv-treated SKOV3 and D5) or CM of parental tumor cell lines (SKOV3 and B16). Consistent with previous research, T cells activated using agonistic anti-CD3 and anti-CD28 antibodies that mimic activation through the T cell receptor (TCR) (hereafter activated) and cultured in aneuploid CM had diminished production of IFN-γ compared to those cultured in diploid CM (Figure 2a, 2b). T cells activated in the presence of aneuploid CM also had a lower proportion of Granzyme B positive cells, suggesting that aneuploid CM decreases cytotoxicity in surrounding T cells (Figure 2b). To investigate if UPR induction was a primary mechanism of T cell dysfunction in this context, $CD3^+$ T cells were activated in the presence of aneuploid CM and the IRE1 inhibitor 4μ8C. The addition of 4μ8C to aneuploid CM did not restore T cell function (Figure 2b). In fact, flow cytometry analysis of activated T cells showed that the addition of 4μ8C in aneuploid CM further worsened T cell dysfunction, reducing the percentage of IFN-γ and Granzyme B positive T cells compared to SKOV3 Rv CM alone (Figure 2b).

To further investigate the role of the UPR in T cell dysfunction, we conducted an analysis of the mRNA and protein expression of the UPR pathways in T cells activated in aneuploid CM. Analysis of mRNA expression of UPR genes revealed that CD3 T cells activated in the presence of aneuploid CM did not have an elevated UPR. Instead, mRNA expression of the IRE1 and PERK pathways was diminished (Figure 2c, 2d). Analysis of T cell lysate also shows that aneuploid CM appears to diminish IRE1 and PERK pathway activity (Figure 2e, 2f).

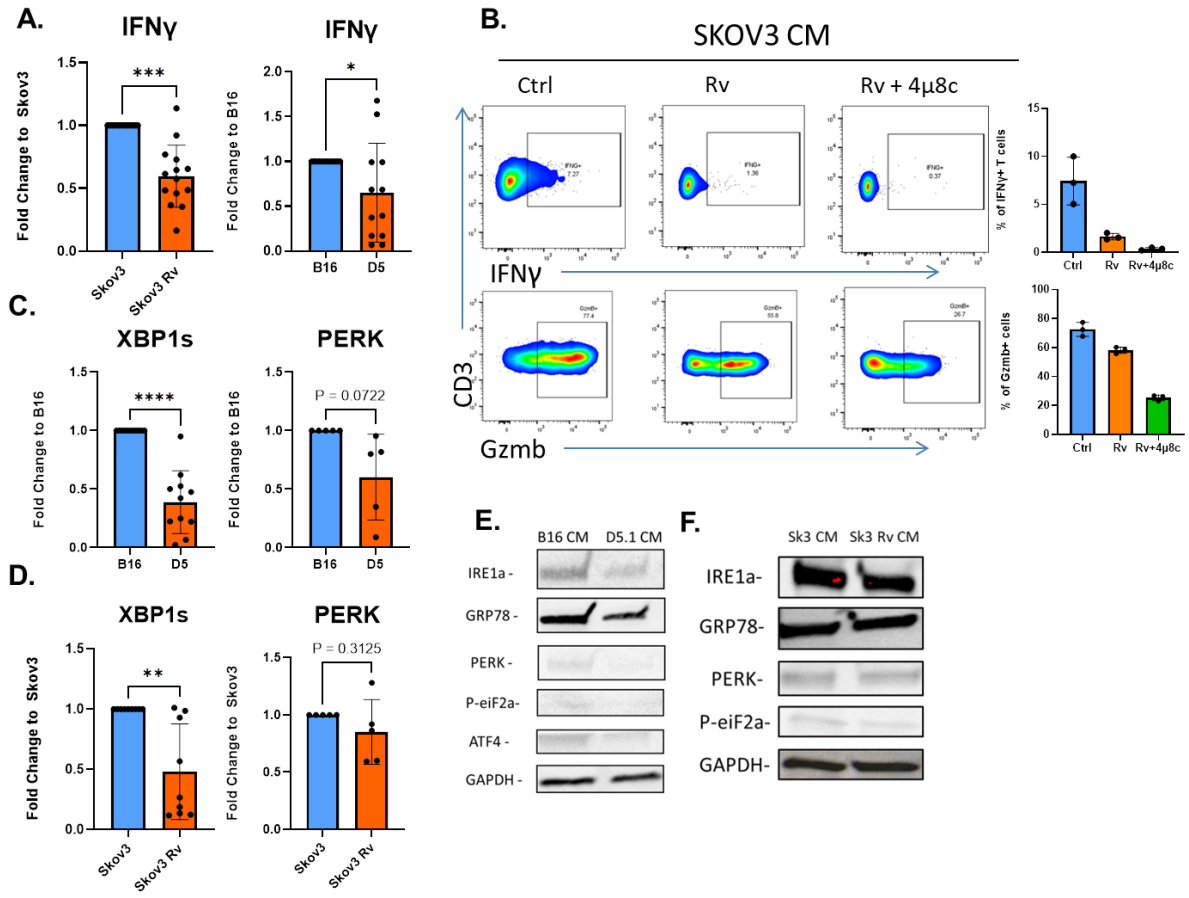

Figure 2**: UPR is diminished in CD3 T cells activated in the presence of aneuploid CM**

(A) Normalized mRNA expression relative to diploid CM condition of IFN-γ in T cells activated by anti-CD3/28 antibodies in the presence of diploid SKOV3 and B16 control CM or aneuploid SKOV3 Rv, D5 CM. (B) Flow cytometry analysis of IFN-γ production (top) and Granzyme B (bottom) in T cells activated in vitro by anti-CD3/28 antibodies in the presence of diploid SKOV3 CM or aneuploid SKOV3 Rv CM ± 4μ8C. Bar graphs represent % of IFN-γ positive T cells (top) or Granzyme B (bottom) T cells. (C) Normalized mRNA expression of IRE1 and PERK pathway in T cells activated by anti-CD3/28 antibodies in the presence of diploid B16 or aneuploid D5 CM. (D) Normalized mRNA expression UPR associated genes in T cells activated by anti-CD3/28 in the presence of diploid SKOV3 or aneuploid SKOV3 Rv CM. (E-F) Western Blot analysis comparing IRE1, PERK protein expression in T cells activated by anti-CD3/28 in the presence of SKOV3 aneuploid CM (E) or D5 CM. Beta actin was used as an endogenous control. All points in bar graphs refer to triplicate experiments expressed as mean ± SD using T cells derived from unique donor PBMCs. Error bars are representative of mean ± 1 SD. All P values are calculated by Wilcoxon matched-pairs signed rank test. * $p \leq 0.05$, ** $p \leq 0.01$, *** $p \leq 0.001$, **** $p \leq 0.0001$.

Acknowledgements

Chapter 2 contains unpublished material coauthored with Magalie Dosset, Gonzalo Almanza, Maurizio Zanetti, Su Xian and Hannah Carter. Flow cytometer machine operation for flow cytometry samples were run by Dennis Young of the Moores Cancer Flow Cytometry Core. Figures displaying experiments with T cells treated by B16 and D5 CM partially consist of experimental data generated by Magalie Dosset, PhD. The final presented figure is a combination of Magalie Dosset's data with my experimental data. The thesis author was the primary author of this chapter.

Chapter 3 INDUCTION OF UPR ACTIVATES T CELLS

Because the onset of reduced function in T cells appeared to correspond with reduction in UPR gene expression, we investigated whether UPR activation can promote T cell function independently of TCR stimulation. To this end, we treated donor PBMC derived T cells to ER stress with Thapsigargin (Tg), a Sarco/Endoplasmic Reticulum Ca^{2+} -ATPase (SERCA-ATPase) inhibitor that is known to induce ER stress and UPR in eukaryotic cells. As expected, the addition of Tg caused strong induction of UPR in T cells, as evidenced by the significant increase in XBP1 splicing (Figure 3d). T cells cultured in the presence of Tg also had significantly increased expression of IFN-γ mRNA expression compared to the untreated condition (Figure 3a). This suggests that the induction of UPR fosters T cell activation and cytokine production. To test if T cells respond similarly when ER stress was induced through transmissible ER stress factors. B16 and SKOV3 tumor cells were treated by Tg to generate TERS CM, as described in Material and Methods. T cells were then cultured in the TERS B16 CM and TERS SKOV3 CM. Similar to the results with Tg, T cells cultured in TERS CM showed increased induction of IFN-γ and increased UPR, though notably the effect of TERS is less potent than that of Tg (Figure 3b). This data suggests that the induction of the UPR is capable of partially activating T cells and is a positive contributor to T cell function in absence of direct TCR activation (Figure 3).

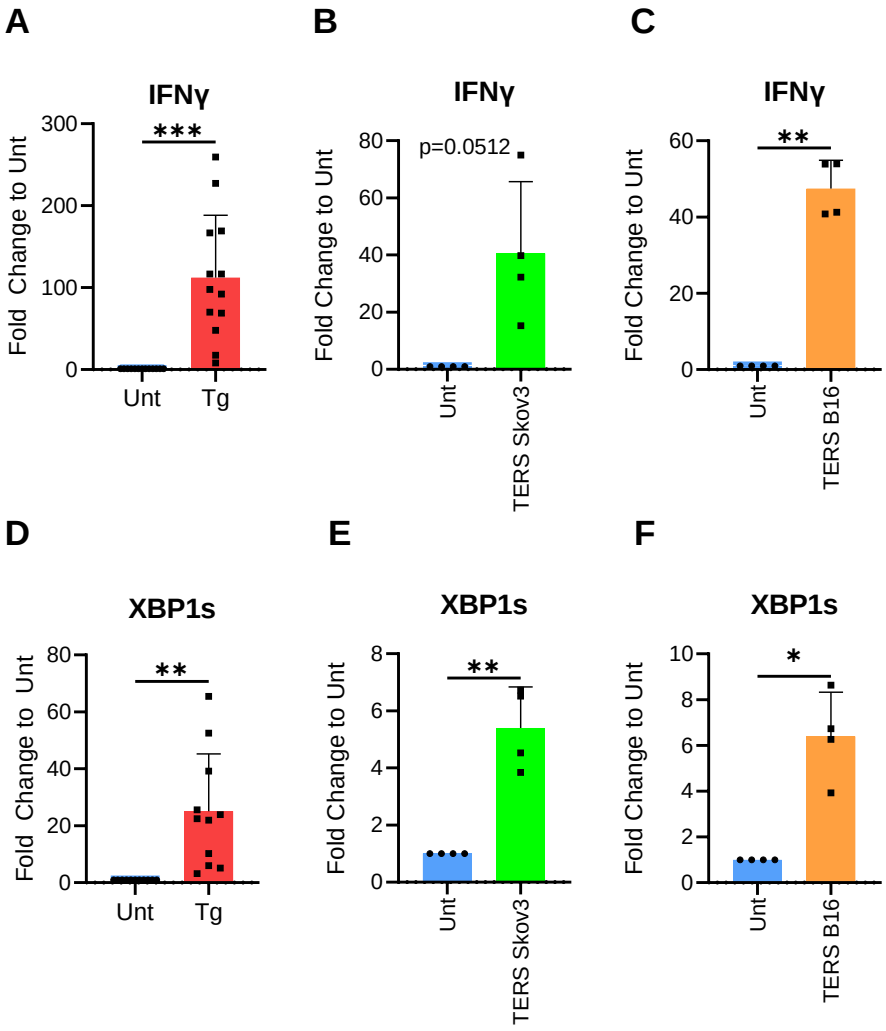

Figure 3: **Induction of ER stress and UPR activates T cells**

(A-C) Normalized mRNA expression of IFN-γ in T cells cultured in medium mixed with 0.3 µM Tg (A) or TERS CM (B-C). (D-F) Normalized mRNA expression relative to untreated of XBP1s in T cells cultured in medium mixed with 0.3 µM Tg (D) or TERS CM (E-F) Beta actin was used as an endogenous control. All points in bar graphs refer to triplicate experiments expressed as mean ± SD. P values were calculated with Wilcoxon matched-pairs signed rank test: * $p \leq 0.05$, ** $p \leq 0.01$, *** $p \leq 0.001$, **** $p \leq 0.0001$. Errors bars represent mean ± 1 SD.

Next, we explore the impact of UPR activation on T cells during conventional TCR activation. First, we tested if the UPR was modulated in T cells activated by anti-CD3/28 antibodies. We found that TCR activation in T cells led to increased splicing of XBP1 and, as expected, IFN-γ, suggesting that the UPR may be involved in the response to TCR activation (Figure 4a). Furthermore, T cells activated by anti-CD3/28 in the presence of Tg showed enhanced expression of IFN-γ compared to the control condition where T cells were activated by anti-CD3/28 alone (Figure 4c). Comparable results were found by culturing activated T cells with TERS CM (Figure 4d-e).

As the addition of the IRE1 inhibitor 4μ8c aggravated T cell dysfunction when mixed with aneuploid CM, I also investigated if induction of the IRE1 pathway could restore T cell function. In order to investigate this, I supplemented the aneuploid CM with IXA4 (10 μM), a specific IRE1/XBP1s activator. The addition of IXA4 was unable to restore IFN-γ expression of T cells cultured in aneuploid CM (Figure 5a), despite induction of XBP1 splicing (Figure 5b). The RIDD pathway also was not significantly altered by aneuploid CM or IXA4 supplementation (Figure 5c). Collectively, the results suggest that aneuploid cancer cells do not transmit an elevated UPR profile to T cells that results in T cell dysfunction. Instead, the data would suggest that the CM of aneuploid cancer cells confers a reduced UPR profile to dysfunctional T cells. However, chemical induction of the IRE1/XBP1s arm is also unable to restore T cell function (Figure 5). Collectively, this data suggests that the induction of the UPR, both chemically and through transmissible ER stress factors, enhances the function of activated T cells. This further supports that the hypothesis that aneuploid cancer cells use transmissible ER stress as a mechanism to confer dysfunction to T cells is refuted. Therefore, the primary mechanism behind the observed diminishment of T cell function is not the result of a TERS

phenomenon or solely due to altered induction of the UPR in T cells. Instead the dysfunction in T cells is the result of unknown alterations caused by the unknown factors in the secretome of aneuploid cancer cells.

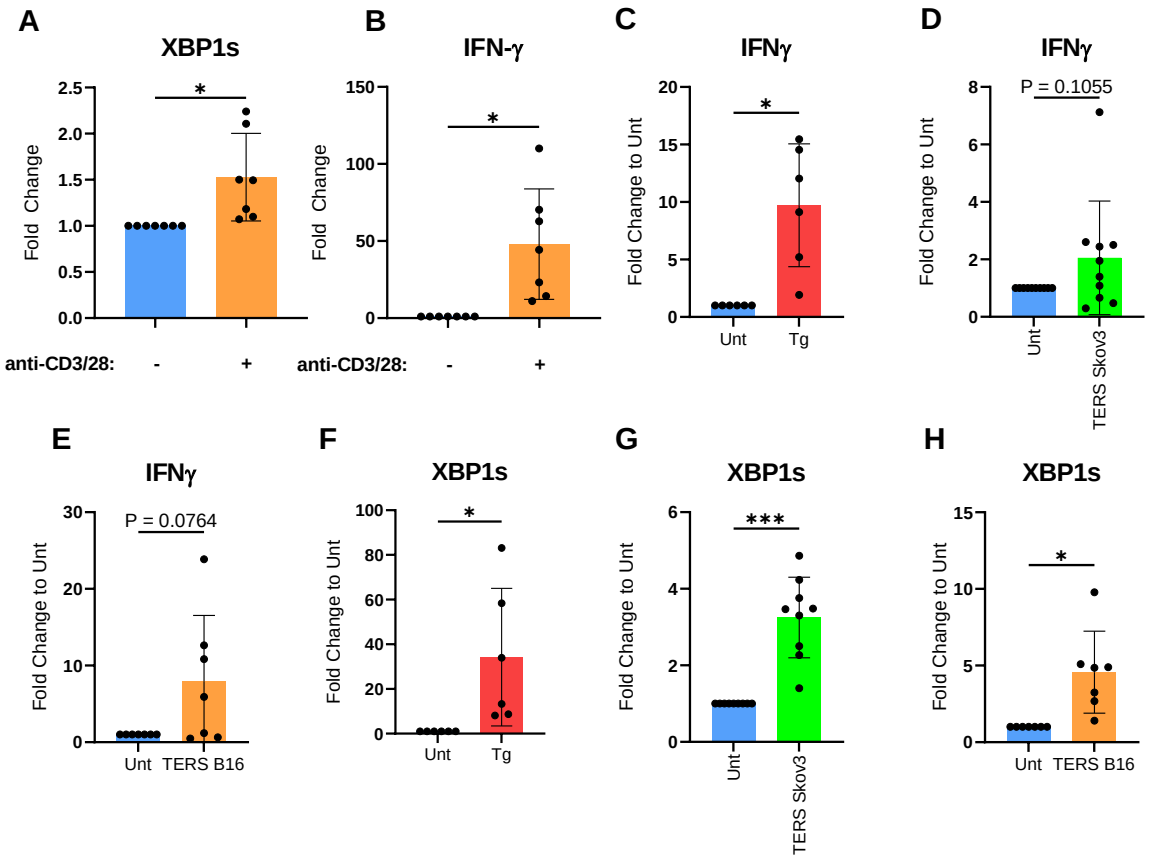

Figure 4: **Induction of UPR enhances T cell activation**

(A-B) Normalized mRNA expression of XBP1s (A) and IFN-γ of T cells activated by anti-CD3/28 antibodies. (C-E) Normalized mRNA expression of IFN-γ of T cells cultured in the presence of 0.3 μM Tg (C) or TERS CM (D-E) antibodies. (F-G) Normalized mRNA expression of XBP1s of T cells activated by anti-CD3/28 antibodies cultured in the presence of Tg (F) or TERS CM (G-H). T cells were activated with anti-CD3/28 antibodies simultaneously with treatment of experimental media. Beta actin was used as an endogenous control. All points in bar graphs refer to triplicate experiments expressed as mean ± SD using T cells derived from unique donor PBMCs. Error bars are representative of mean ± 1 SD. All P values are calculated by Wilcoxon matched-pairs signed rank test.

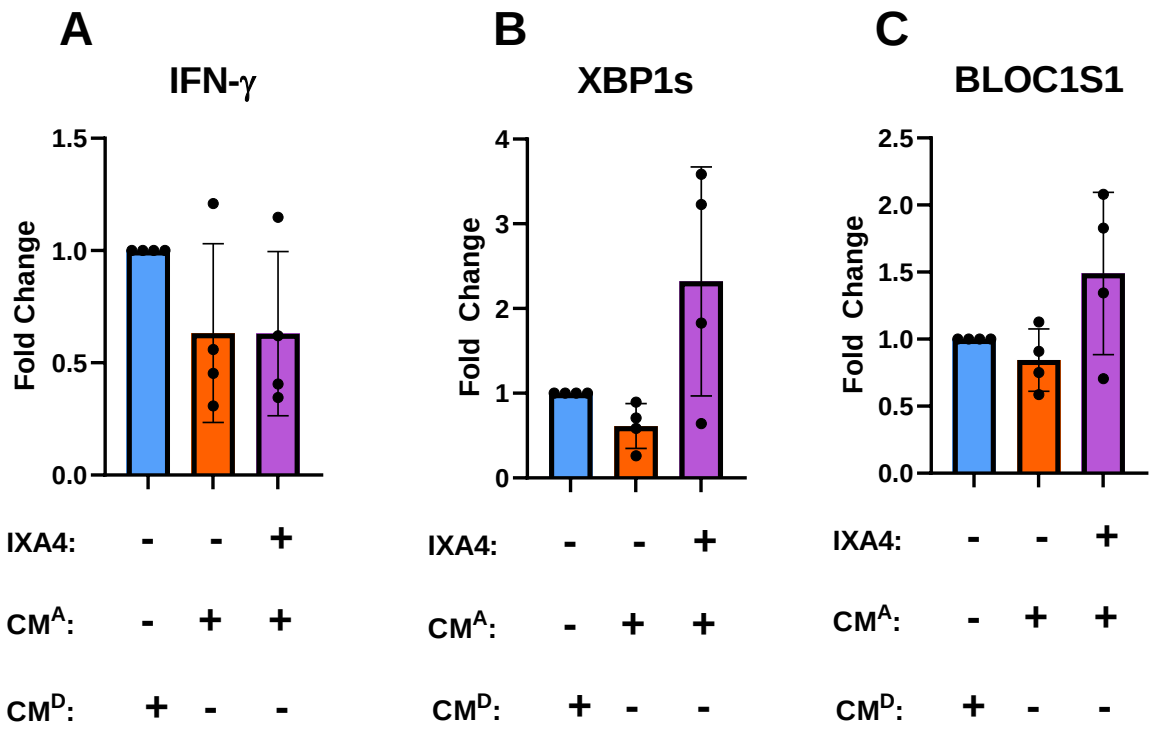

Figure 5: **Agonism of the IRE1 pathway is unable to restore T cell function**

(A) Normalized mRNA expression of IFN-γ in activated T cells cultured in Skov3 CM (CM^D) or aneuploid Skov3 Rv CM (CM^A) ± IXA4 (10 uM). Points on bar graphs represent triplicate averages of unique donor PBMCs. (B) Normalized mRNA expression of XBP1s in activated T cells cultured in Skov3 CM (CM^D) or aneuploid Skov3 Rv CM (CM^A) ± IXA4. (C) Normalized mRNA expression of BLOC1S1 in activated T cells cultured in Skov3 CM (CM^D) or aneuploid Skov3 Rv CM (CM^A) ± IXA4 (10 uM). All points in bar graphs refer to triplicate experiments expressed as mean ± SD using T cells derived from unique donor PBMCs. Error bars are representative of mean ± 1 SD. All P values are calculated by Wilcoxon matched-pairs signed rank test.

Acknowledgements

Chapter 3 contains unpublished material coauthored with Magalie Dosset, Gonzalo Almanza, Maurizio Zanetti, Su Xian, and Hannah Carter. The thesis author was the primary author of this chapter.

Chapter 4 EFFECT OF ANUEPLOID CM ON T CELL METABOLISM

In addition to ER stress and UPR, we also investigated alternative mechanisms to explain the observed T cell dysfunction. T cells require significant metabolic resources for proper function and upon activation switch to glycolysis from oxidative phosphorylation (OXPHOS), even in aerobic conditions with sufficient oxygen for OXPHOS (Bental et. al, 1993, Fox et al., 2005). Zhao et al., found that ovarian cancer imposed glucose restriction which increased expression of microRNAs that inhibit expression of EZH2 (Zhao et al., 2018). EZH2 promotes T cell survival and polyfunctional cytokine expression via Bcl-2 signaling (Zhao et al, 2018). Accordingly, T cells dysfunction manifests in a loss of polyfunctionality and increased apoptosis (Zhao et al., 2018). Therefore, we investigated the possibility that the aneuploid cancer cells impair EZH2 expression by imposing glucose restriction on T cells.

In activated T cells cultured in the presence of aneuploid CM we observed a clear reduction of EZH2 expression compared to T cells cultured in diploid CM (Figure 6a, 6b). There was also a moderate correlation between EZH2 and IFN-γ expression in T cells cultured in either aneuploid or diploid CM, suggesting reduction of EZH2 as a potential mechanism behind the dysfunctional phenotypes observed in T cells activated in the presence of aneuploid CM. (Figure 6c, Figure 6d). To test if a glucose restriction in aneuploid CM may be the cause of T cell dysfunction, activated T cells were cultured in aneuploid D5 CM supplemented with 2 mg/mL of glucose. The addition of glucose to aneuploid D5 CM was able to partially restore IFN-γ production (Figure 6e). This suggests that aneuploid tumor cells uptake more glucose from the microenvironment and that aneuploid CM may leverage glucose restriction as a mechanism to impair T cell function, possibly through inhibition of EZH2 (Figure 6e).

As the inhibition of IRE1 pathway via supplementing the CM with 4μ8c appeared to aggravate T cell dysfunction, we attempted to investigate the effect of specific induction of the IRE1 pathway on T cell function in the presence of aneuploid CM and also see if the restoring effect of glucose on T cells seen in chapter 4 could be amplified by combining it with induction of the IRE1 pathway. To test this, we cultured T cells for 2 days in aneuploid CM supplemented with glucose (2 mg/mL) and IXA4 (10 μM) a specific IRE1/XPB1s activator. However, the addition of both glucose and IXA4 did not amplify the restorative effect of glucose on T cell function (Figure 7a, 7d). Consistent with figure 3, addition of only IXA4 to aneuploid CM did not significantly alter the production of IFN-γ in T cells (Figure 3a, 7a, 7d). Therefore, it would appear that while inhibition of the IRE1 pathway aggravates dysfunction caused by aneuploid CM, the induction of the IRE1 pathway alone is insufficient to reverse the effect of aneuploid CM on T cell function (Figure 7).

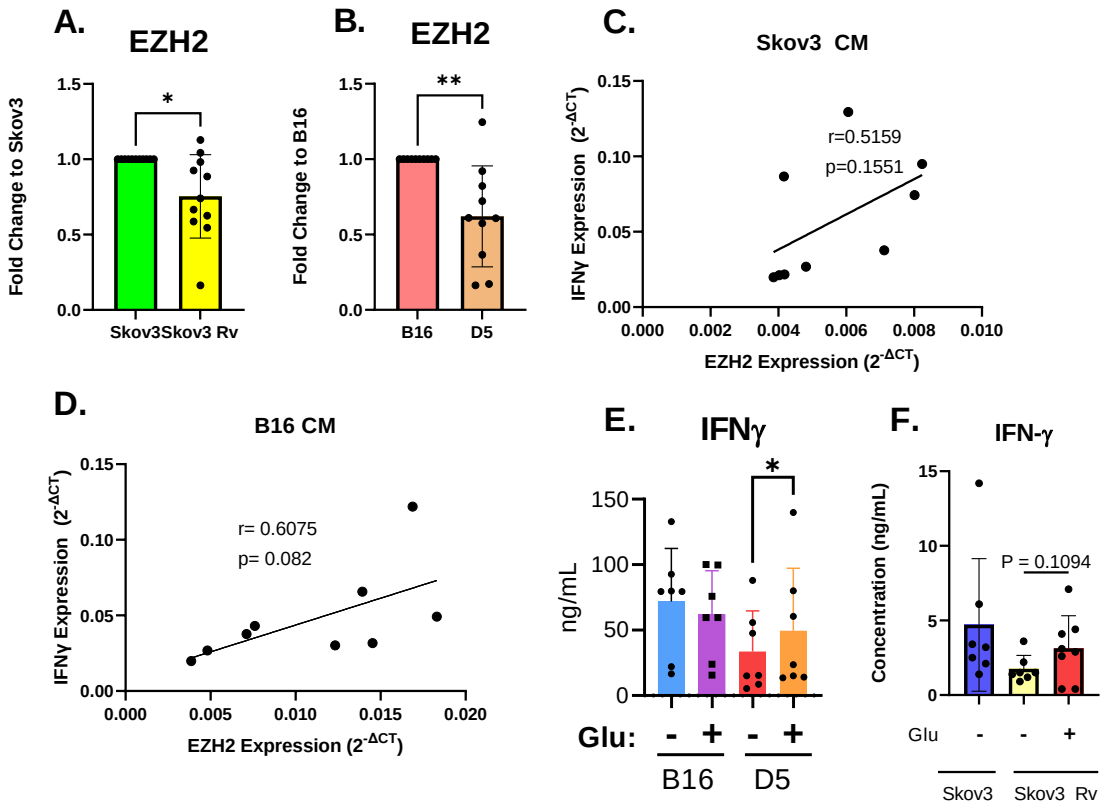

Figure 6: **Aneuploid CM reduces EZH2 expression in dysfunctional T cells**

(A-B) Normalized mRNA expression of EZH2 in T cells activated by anti-CD3/28 antibodies cultured in the presence of aneuploid SKOV3 Rv CM or aneuploid D5 CM. (C-D) Scatter charts comparing EZH2 expression to IFN-γ expression in activated T cells cultured in CM. R values are Spearman coefficients. (E-F) IFN-γ production of T cells cultured in B16 or D5 CM ± Glucose (2 mg/ml) (E) or Skov3 Rv CM (F) measured by ELISA. All dots on bar graphs represent triplicate experiments expressed as mean and bar graphs are represented as mean ± SD. Error bars are representative of mean ± 1 SD. P values are calculated with Wilcoxon matched-pairs signed rank test. * $p \leq 0.05$, ** $p \leq 0.01$, *** $p \leq 0.001$, **** $p \leq 0.0001$.

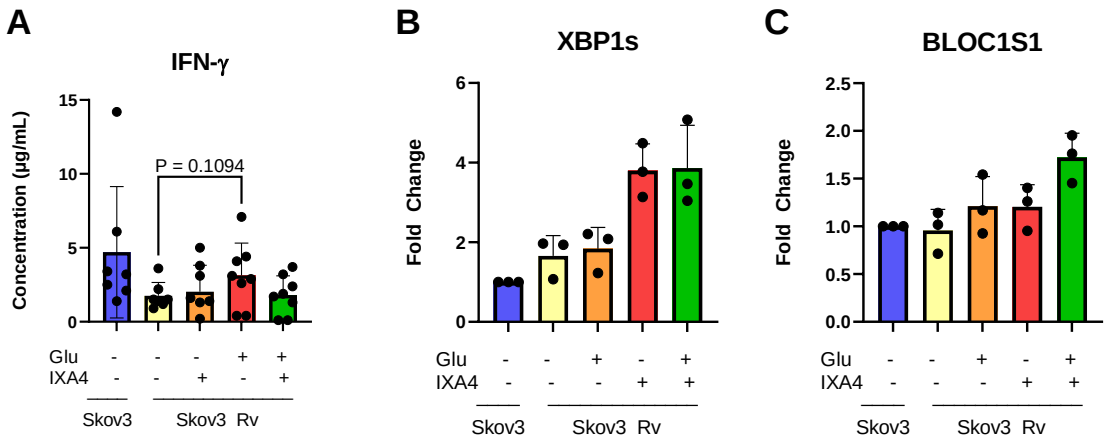

Figure 7: **The supplementation of IXA4 to Aneuploid CM does not restore T cell function**

(A) Normalized mRNA expression of IFN-γ in T cells activated by anti-CD3/28 antibodies cultured in the presence of aneuploid SKOV3 Rv CM ± IXA4 (10 µM) and Glucose (2 mg/mL). (B-C) Normalized mRNA expression of XBP1s (B) and BLOC1S1 (C) in T cells activated by anti-CD3/28 antibodies cultured in the presence of aneuploid SKOV3 Rv CM ± IXA4 (10 µM) and Glucose (2 mg/mL). (D) IFN-γ production measured by ELISA of T cells activated by anti-CD3/28 antibodies and cultured in the presence of aneuploid SKOV3 Rv CM ± IXA4 (10 µM) and Glucose (2 mg/mL). All points represent triplicate experiments with expressed as mean and bar graphs are represented as mean ± SD. Error bars are representative of mean ± 1 SD. P values are calculated with Wilcoxon matched-pairs signed rank test. * $p \leq 0.05$, ** $p \leq 0.01$, *** $p \leq 0.001$, **** $p \leq 0.0001$.

Acknowledgements:

Chapter 4 contains unpublished material coauthored with Magalie Dosset, Gonzalo Almanza, Maurizio Zanetti, Su Xian, and Hannah Carter. Magalie Dosset performed the ELISA assay shown in figure 6e while I assisted with the cell treatment. The thesis author was the primary author of this chapter.

Chapter 5 DISCUSSION

This study sought to test the hypothesis that aneuploidy in cancer cells induced a transmissible UPR that conferred an elevated UPR and subsequent dysfunction in T cells (Zanetti, 2017). The results show that the CM of aneuploid cancer cells conferred decreased T cell function and cytotoxicity compared to the CM of diploid cancer cells. This suggests that aneuploidy in cancer cells can gain a survival advantage by becoming less susceptible to immune surveillance. In addition, the fact that the aneuploid CM alone is capable of conferring dysfunction to T cells supports the hypothesis that the mechanistic link between aneuploidy and reduced immune surveillance is cell-nonautonomous and therefore due to some alteration in the secretome of aneuploid cancer cells. These results are in line with our initial hypothesis regarding the immunosuppressive potential of tumor aneuploidy and have been replicated previously by other researchers (Xian et al., 2021, Mahadevan et. al., 2011). However, T cells that become dysfunctional in the presence of aneuploid CM have a diminished UPR. The addition of UPR inhibitors does not restore T cell function (Figure 2). In addition, D5 and SKOV3 Rv aneuploid cancer cells appear to have diminished UPR compared to the parental SKOV3 and B16 cell lines refuting the hypothesis that aneuploidy induces UPR in cancer cells and a transmissible ER stress phenotype (Figure 1b). Therefore, the assumption that TERS mechanistically links aneuploidy and T cell dysfunction is not supported by these studies.

While ER stress and sustained UPR have been documented in cancer cells, there is less evidence that the induction of aneuploidy in cancer cells can induce a sustained elevation of the UPR (Madden et. al., 2018). The induction of aneuploidy via cell-to-cell fusion in yeast cells was reported to increase client protein dosages (Torres et. al., 2007), but the results of this study

could not find evidence that the D5, a cell model of cancer aneuploidy due to cell-in-cell fusion, had increased UPR (Figure 1b). Previous research also found that SKOV3 treated with Reversine led to increased splicing of XBP1 (Xian et. al., 2021), results at variance with the findings of this study where SKOV3 treated with Reversine showed diminished spliced XBP1 mRNA (Figure 1c). This finding could be explained by the fact that SKOV3 cells treated with Reversine were analyzed up to 14 days after treatment removal, while the cells were collected right after 3 days of treatment with no resting period in the Xian et al. study (Xian et. al., 2021). It is also possible that the induction of aneuploidy in cancer cells may induce extremely strong ER stress that quickly activates the apoptotic response in the UPR. The UPR is beneficial below a certain threshold of ER stress; however past this threshold, the UPR has been documented to switch from an adaptive survival response to that of an apoptotic response (Szegezdi et. al., 2006). Therefore, the only surviving aneuploid cells are those that downregulate elements of the UPR in order to prevent apoptotic responses to survive

The inhibition of IRE1 pathway by 4μ8C not only fails to counteract the reduction of IFN-γ by aneuploid CM but appears to aggravate the dysfunctional T cell phenotype (Figure 2b). This is in contradiction with research by other groups that have implicated IRE1-XBP1 pathway activity with T cell dysfunction in cancer contexts (Song et. al., 2018, Riesenberg et al., 2023). Song et. al., found that the ascites fluid of ovarian cancer patients caused increased IRE1-XBP1 activity and suppressed IFN-γ production in stark contrast to the findings of this study where suppressed IFN-γ induction was associated with lowered XBP1s expression (Figure 2). Riesenberg et al. also found that T cells in murine and human cancer models experience hyperactive IRE1 signaling that is detrimental to T cell mediated tumor control, but also found that specific induction of the adaptive arm of IRE1 with IXA4 protected T cells from the effects

of chronic ER stress (Riesenberg et al., 2023). However, the dysfunctional T cells observed in the present study did not demonstrate hyperactivity in any of the branches of the UPR (Figure 2c-d) and enforced XBP1 splicing by IXA4 did not significantly restore or inhibit T cell function in the presence of aneuploid CM (Figure 7). Therefore, while T cell dysfunction caused by hyperactive IRE1-XBP1 activity may be present in certain cancer contexts, the modulation of the UPR is not a primary the driving mechanism connecting cancer aneuploidy and T cell dysfunction.

In addition to reductions in UPR, T cells made dysfunctional by aneuploid CM also showed a significant reduction in EZH2 expression that correlated with a reduction in IFN-γ expression. The ablation of EZH2 has been previously observed to compromise effector CD8 T cell function in both acute infection and cancer models (Zhao et al., 2016, Chen et al., 2018). In cancer models several reports found that tumor supernatant impaired CD8 T lymphocyte function through miR-26a mediated inhibition of EZH2 (Zhao et al., 2016, Long et al., 2016). The data presented herein corroborate these earlier findings in a novel context, in which the induction of aneuploidy results in the development of a secretome that significantly inhibits EZH2 expression in T cells. The present experiments also suggest that glucose restriction in the secretome partially contributes to the immunosuppressive potential of aneuploid cancer cells, indicating that aneuploid cancer cells may deplete glucose content more rapidly compared to their diploid counterparts (Figure 6). However, it is unknown if this glucose restriction causes dysfunction in T cells via EZH2 inhibition, as Zhao et al. (Zhao et al., 2018) suggests is the primary mechanism of EHZ2 inhibition, or if the glucose restriction and EZH2 function independently to cause dysfunction and are governed by distinct mechanisms. Despite IRE1 inhibition being detrimental to T cell function in the context of the aneuploid secretome, the

combination of glucose and IXA4 supplementation to aneuploid CM did not yield any improvement of IFN-γ production in T cells.

Table 1: **Reagents and Resources Table**

Reagents/Resources	Reference or Source	Identifier or Cat. No.
Chemicals and Cytokines		
Reversine	Selleck Chem	S7588
Thapsigargin	Tocris	1138
4μ8c	Sigma	SML0949
D-Glucose	Gibco	A2494001
Halt™ Protease Inhibitor Cocktail	Thermo Scientific	78429
IXA4	MedChemExpress	HY-139214
Cell Lines		
SKOV3	ATCC	CCL-221
B16.F10	ATCC	CRL-6475
D5 Polyploidy Cells	(Searles et al., 2018)	
Antibodies		
BV711 anti-human CD3	Biolegend	300328
PerCP/Cy5.5 anti-human CD45RO	Biolegend	304222
PE anti-human IFN-γ	Biolegend	502509
PE-dazzle anti-human CD69	Biolegend	310924
Alexa-Fluor 647 anti-human granzyme B	Biolegend	515406
Fixable Viability Dye eFluor 780	Thermo Fisher Scientific	65-0865-14
ATF4 (C-20) antibody	Santa Cruz	sc-200
IRE1a (14C10) antibody	Cell Signaling	3294
GAPDH	Santa Cruz	sc-20358
GRP78/BIP antibody	BD Bioscience	610978
PERK (C33E10) antibody	Cell Signaling	3192
phospho-eif2a (D9G8)	Cell Signaling	3398
Rabbit IgG-HRP antibody	Cell Signaling	7074
Mouse IgGκ	Santa Cruz	sc-516102
Donkey anti-goat IgG HRP	Santa Cruz	sc-2020
Alexa-Fluor 488 mouse anti-human CD8	BD Bioscience	344716
BV605 mouse anti-human CD279	BD Bioscience	563245
Oligonucleotides		
XBP1 forward proprietary	Thermo Fisher Scientific	Cat no. 4331182 Assay Hs00231936_m1
XBP1 reverse proprietary	Thermo Fisher Scientific	Cat no. 4331182 Assay Hs00231936_m1
eif2ak3 forward proprietary	Thermo Fisher Scientific	Cat no.4331182 Assay Hs00984003_m1
eif2ak3 reverse proprietary	Thermo Fisher Scientific	Cat no.4331182 Assay Hs00984003_m1

Table 2: **Reagents and Resources Continued**

Reagents/Resources	Reference or Source	Identifier or Cat. No.
Oligonucleotides		
Ifngr2 forward proprietary	Thermo Fisher Scientific	Cat no.4331182 Assay Hs00194264_m1
Ifngr2 reverse proprietary	Thermo Fisher Scientific	Cat no.4331182 Assay Hs00194264_m1
ACTB forward proprietary	Thermo Fisher Scientific	Cat no.4331182 Assay Hs01060665_g1
ACTB reverse proprietary	Thermo Fisher Scientific	Cat no.4331182 Assay Hs01060665_g1
EZH2 forward proprietary	Thermo Fisher Scientific	Cat no.4331182 Assay Hs00544830_m1
EZH2 reverse proprietary	Thermo Fisher Scientific	Cat no.4331182 Assay Hs00544830_m1

Cell Lines and Cell Culture Conditions:

Cells were cultured in culture medium supplemented with 5% FBS from Atlanta Biologics, 1X Gibco pencillin-streptomycin-glutamine, 1mM Corning Sodium Pyruvate, 1X Gibco MEM Non-Essential Amino Acids, Gibco HEPES. B16.F10 and D5 (Murine Melanoma) cells were cultured in Gibo RPMI-1640 medium while SKOV3 and SKOV3 Rv (Human Ovarian Carcinoma) cells were cultured in DMEM medium, both supplemented with the previously listed reagents. SKOV3 and B16.F10 were purchased from ATCC 5% CO_2. D5 fused cells were a gift from Stephen Searles and were maintained in RPM-1640 complete medium. All cells were cultured at 37° Celsius, passaged bi-weekly and treated with Plasmocin® (InvivoGen) for 2 weeks on a monthly basis to prevent mycoplasma contamination.

Induction of Aneuploidy and CM generation:

Aneuploid SKOV3 Rv cells were generated by treating SKOV3 cells with reversine (2 μM) for 2 days in a T75 flask at an initial starting density of 2E5 cells. After reversine treatment cells were washed with PBS 2x and cell culture medium replaced with fresh complete cell culture medium. New aneuploid SKOV3 Rv cells were generated every 2 weeks using the previously described method; previous SKOV3 Rv cells were discarded. New D5 cells that were not derived from cells in culture were generated by Limited Dilution Cloning of original D5 cells gifted by Stephen Searles (Searles et al., 2018). CM was harvested from aneuploid cells after cell density reached ~3.5 million cells per T75 flask. CM was spun at 2000 RPM for 5 minutes to separate debris and then decanted into 1.5 mL Eppendorf tubes. The addition of any additional reagent supplementation to the CM was done on the day of the experiment and any excess CM mixture was discarded. CM was stored at -80° Celsius when not in use.

Transmissible ER Stress Phenotype and CM generation:

TERS cancer cell phenotypes were generated with the protocol previously described by Mahadevan et al. (Mahadevan et al., 2012). Skov3 and B16 cells were treated with Tg (0.3μM) for 2 hours at 37° Celsius, washed with PBS 2x and allowed to rest in fresh complete culture medium at 37° Celsius for 1 day. CM was harvested and spun at 2000 RPM for 5 minutes to separate any debris before being decanted into 1.5 mL Eppendorf tubes. CM was stored at -80° Celsius when not in use. TERS cells were not reused after CM was collected.

T cell treatment:

T cells were isolated from donor PBMCs using an EasySep™ CD3 Positive Selection Kit (Stemcell™ Technologies) according to manufacturer protocols. T cells were cultured in 96 well plates at 2E5 cells per well and activated with coated anti-CD3/28 antibodies. Anti-CD3/28 antibodies were prepared at 2 µg/ml and allowed to adhere to wells for 2 hours at 37° Celsius. T cells were activated at the same time as treatment with CM or other experimental media. T cells treated with Tg (0.3 µM) or TERS CM were treated for 1 day while T cells treated with aneuploid CM were treated for 2 days. After treatment, T cells were harvested for analysis and the T cell CM stored.

RNA Extraction and cDNA synthesis:

Cells used for RT-PCR were lysed in RA1 (Machery-Nagel) lysis buffer to prepare for RNA extraction. RNA extraction was conducted with a NucleoSpin® RNA purification kit according to manufacturer protocols. RNA concentration and purity were quantified using a spectrophotometer (ND-1000) and analyzed with NanoDrop Software v3.8.0. RNA was normalized between conditions and cDNA was generated with a high-capacity cDNA reverse transcription kit (Applied Biosystems™)

RT-qPCR:

RT-qPCR was performed on cDNA using an ABI 7300 Real-Time PCR system and Taqman reagents for 40 cycles under universal cycling conditions. Cycling conditions followed manufacturer's specifications. Target gene expression was normalized to Beta actin and relative

expression was determined using the $2^{-\Delta Ct}$ relative quantification method. Primers were purchased from ThermoFisher Scientific.

Western Blot:

Protein lysates for Western Blotting were prepared in RIPA lysis buffer supplemented with 1x Protease Inhibitor Cocktail (Thermo Scientific). Lysate samples were measured and normalized for protein concentrations with a Pierce™ BCA Protein Assay Kit. Gels were transferred onto nitrocellulose membranes using a Bio-Rad Trans-Blot Turbo transfer system. Membranes were saturated in TBS tween 0.1%, 5% milk powder for 1 hour and washed in TBS tween 0.1% 3x before primary antibody blotting overnight at 4° on a plate shaker. Membranes were washed 3x in TBS tween 0.1% before secondary antibody blotting for 1 hour. All antibody dilutions were according to manufacturer specifications.

IFN-γ ELISA:

IFN-γ concentrations were measured using an ELISA MAX Deluxe Set Human IFN-γ kit (BioLegend®) according to manufacturer protocols. 1M sulfuric acid served as a stop solution. Absorbance was read at 450 nm.

Flow Cytometry:

T cells used in flow cytometry analysis were first stained extracellularly with specific antibodies against CD3, CD4, CD8, CD45RO, CD69, PD1, and fixed viability dye, before intracellular staining with antibodies against IFN-γ and Granzyme B. FACS reading was done on a BD FACSAria™ II and data analyzed using Flowjo.

Mice Protocols:

C57BL6 mice were grafted with B16 (0.2 million cells) or D5 (1 million cells) prepared in 100 µL of PBS 1x via subcutaneous injection on the right flank. Tumors were allowed to grow until they reached ~100 mm^2 and then harvested. TILs were isolated from tumors using Percoll gradient separation. Mice housing, care, and use all adhered to the University of California policy.

REFERENCES

Bleackley, R. C., Duggan, B., Ehrman, N., & Lobe, C. G. (1988). Isolation of two cDNA sequences which encode cytotoxic cell proteases. FEBS Letters, 234(1), 153–159. https://doi.org/10.1016/0014-5793(88)81323-1

Boveri T. Concerning the origin of malignant tumours by Theodor Boveri. Translated and annotated by Henry Harris. J Cell Sci. 2008 Jan;121 Suppl 1:1-84. doi: 10.1242/jcs.025742. PMID: 18089652.

Beroukhim R, Mermel CH, Porter D, Wei G, Raychaudhuri S, Donovan J, Barretina J, Boehm JS, Dobson J, Urashima M, Mc Henry KT, Pinchback RM, Ligon AH, Cho YJ, Haery L, Greulich H, Reich M, Winckler W, Lawrence MS, Weir BA, Tanaka KE, Chiang DY, Bass AJ, Loo A, Hoffman C, Prensner J, Liefeld T, Gao Q, Yecies D, Signoretti S, Maher E, Kaye FJ, Sasaki H, Tepper JE, Fletcher JA, Tabernero J, Baselga J, Tsao MS, Demichelis F, Rubin MA, Janne PA, Daly MJ, Nucera C, Levine RL, Ebert BL, Gabriel S, Rustgi AK, Antonescu CR, Ladanyi M, Letai A, Garraway LA, Loda M, Beer DG, True LD, Okamoto A, Pomeroy SL, Singer S, Golub TR, Lander ES, Getz G, Sellers WR, Meyerson M. The landscape of somatic copy-number alteration across human cancers. Nature. 2010 Feb 18;463(7283):899-905. doi: 10.1038/nature08822. PMID: 20164920; PMCID: PMC2826709.

Chen, X., Cubillos-Ruiz, J.R. Endoplasmic reticulum stress signals in the tumour and its microenvironment. *Nat Rev Cancer* **21**, 71–88 (2021). https://doi.org/10.1038/s41568-020-00312-2

Chen, G., Subedi, K., Chakraborty, S., Sharov, A., Lu, J., Kim, J., Mi, X., Wersto, R., Sung, M.-H., & Weng, N. (2018). Ezh2 Regulates Activation-Induced CD8+ T Cell Cycle Progression via Repressing Cdkn2a and Cdkn1c Expression. Frontiers in Immunology, 9, 549. https://doi.org/10.3389/fimmu.2018.00549

Fenimore, J., Young, H.A. (2016). Regulation of IFN-γ Expression. In: Ma, X. (eds) Regulation of Cytokine Gene Expression in Immunity and Diseases. Advances in Experimental Medicine and Biology, vol 941. Springer, Dordrecht. https://doi.org/10.1007/978-94-024-0921-5_1

Hollien, J., & Weissman, J. S. (2006). Decay of endoplasmic reticulum-localized mRNAs during the unfolded protein response. Science (New York, N.Y.), 313(5783), 104–107. https://doi.org/10.1126/science.1129631

Jorgovanovic, D., Song, M., Wang, L., & Zhang, Y. (2020). Roles of IFN-γ in tumor progression and regression: A review. Biomarker Research, 8(1), 49. https://doi.org/10.1186/s40364-020-00228-x

Kemp, K., & Poe, C. (2019). Stressed: The Unfolded Protein Response in T Cell Development, Activation, and Function. *International Journal of Molecular Sciences*, *20*(7), 1792. https://doi.org/10.3390/ijms20071792

Koumenis C, Wouters BG. "Translating" tumor hypoxia: unfolded protein response (UPR)-dependent and UPR-independent pathways. Mol Cancer Res. 2006 Jul;4(7):423-36. doi: 10.1158/1541-7786.MCR-06-0150. PMID: 16849518.

Liu, C. Y., & Kaufman, R. J. (2003). The unfolded protein response. Journal of Cell Science, 116(10), 1861–1862. https://doi.org/10.1242/jcs.00408

Long, H., Xiang, T., Luo, J., Li, F., Lin, R., Liu, S., Jiang, S., Hu, C., Chen, G., Wong, E., Wan, Y., Li, Q.-J., & Zhu, B. (2016). The tumor microenvironment disarms CD8+ T lymphocyte function via a miR-26a-EZH2 axis. Oncoimmunology, 5(12), e1245267. https://doi.org/10.1080/2162402X.2016.1245267

Mahadevan NR, Anufreichik V, Rodvold JJ, Chiu KT, Sepulveda H, Zanetti M. Cell-extrinsic effects of tumor ER stress imprint myeloid dendritic cells and impair $CD8^+$ T cell priming. PLoS One. 2012;7(12):e51845. doi: 10.1371/journal.pone.0051845. Epub 2012 Dec 18. PMID: 23272178; PMCID: PMC3525659.

Mahadevan NR, Rodvold J, Sepulveda H, Rossi S, Drew AF, Zanetti M. Transmission of endoplasmic reticulum stress and pro-inflammation from tumor cells to myeloid cells. Proc Natl Acad Sci U S A. 2011 Apr 19;108(16):6561-6. doi: 10.1073/pnas.1008942108. Epub 2011 Apr 4. PMID: 21464300; PMCID: PMC3081038. Madden, E., Logue, S. E., Healy, S. J., Manie, S., & Samali, A. (2019). The role of the unfolded protein response in cancer progression: From oncogenesis to chemoresistance. *Biology of the Cell*, *111*(1), 1–17. https://doi.org/10.1111/boc.201800050

Morishima, N., Nakanishi, K., & Nakano, A. (2011). Activating transcription factor-6 (ATF6) mediates apoptosis with reduction of myeloid cell leukemia sequence 1 (Mcl-1) protein via induction of WW domain binding protein 1. The Journal of Biological Chemistry, 286(40), 35227–35235. https://doi.org/10.1074/jbc.M111.233502

Pino, S. C., O'Sullivan-Murphy, B., Lidstone, E. A., Thornley, T. B., Jurczyk, A., Urano, F., Greiner, D. L., Mordes, J. P., Rossini, A. A., & Bortell, R. (2008). Protein kinase C signaling during T cell activation induces the endoplasmic reticulum stress response. *Cell Stress & Chaperones*, *13*(4), 421–434. https://doi.org/10.1007/s12192-008-0038-0

Riesenberg, B. P., Gandy, E. J., Kennedy, A. S., Hunt, E. G., Hurst, K. E., Sedlacek, E. L., Gao, P., Emanuele, M. J., Modliszewski, J., Green, J. M., Milner, J. J., Wiseman, R. L., & Thaxton, J. E. (2023). Adaptive IRE1 Signaling Elicits T Cell Metabolic Remodeling and Tumor Control (p. 2023.11.16.567431). bioRxiv. https://doi.org/10.1101/2023.11.16.567431

Rzymski, T., & Harris, A. L. (2007). The unfolded protein response and integrated stress response to anoxia. Clinical Cancer Research: An Official Journal of the American

Association for Cancer Research, 13(9), 2537–2540. https://doi.org/10.1158/1078-0432.CCR-06-2126

Searles, S., Santosa, E., & Bui, J. D. (2018). Cell-cell fusion as a mechanism of DNA exchange in cancer. The Journal of Immunology, 200(1_Supplement), 56.24. https://doi.org/10.4049/jimmunol.200.Supp.56.24

Shen, J., Chen, X., Hendershot, L., & Prywes, R. (2002). ER stress regulation of ATF6 localization by dissociation of BiP/GRP78 binding and unmasking of Golgi localization signals. Developmental Cell, 3(1), 99–111. https://doi.org/10.1016/s1534-5807(02)00203-4

Schröder M, Kaufman RJ. ER stress and the unfolded protein response. Mutat Res. 2005 Jan 6;569(1-2):29-63. doi: 10.1016/j.mrfmmm.2004.06.056. PMID: 15603751.

Szegezdi, E., Logue, S. E., Gorman, A. M., & Samali, A. (2006). Mediators of endoplasmic reticulum stress-induced apoptosis. EMBO reports, 7(9), 880–885. https://doi.org/10.1038/sj.embor.7400779

Thomas, D. A., & Massagué, J. (2005). TGF-beta directly targets cytotoxic T cell functions during tumor evasion of immune surveillance. Cancer Cell, 8(5), 369–380. https://doi.org/10.1016/j.ccr.2005.10.012

Torres EM, Sokolsky T, Tucker CM, Chan LY, Boselli M, Dunham MJ, Amon A. Effects of aneuploidy on cellular physiology and cell division in haploid yeast. Science. 2007 Aug 17;317(5840):916-24. doi: 10.1126/science.1142210. PMID: 17702937.

Xian S, Dosset M, Almanza G, Searles S, Sahani P, Waller TC, Jepsen K, Carter H, Zanetti M. The unfolded protein response links tumor aneuploidy to local immune dysregulation. EMBO Rep. 2021 Dec 6;22(12):e52509. doi: 10.15252/embr.202152509. Epub 2021 Oct 26. PMID: 34698427; PMCID: PMC8647024.

Yoshida, H., Matsui, T., Yamamoto, A., Okada, T., & Mori, K. (2001). XBP1 mRNA is induced by ATF6 and spliced by IRE1 in response to ER stress to produce a highly active transcription factor. Cell, 107(7), 881–891. https://doi.org/10.1016/s0092-8674(01)00611-0

Zanetti, M. (2017). Chromosomal chaos silences immune surveillance. Science, 355(6322), 249–250. https://doi.org/10.1126/science.aam5331

Zhao, E., Maj, T., Kryczek, I., Li, W., Wu, K., Zhao, L., Wei, S., Crespo, J., Wan, S., Vatan, L., Szeliga, W., Shao, I., Wang, Y., Liu, Y., Varambally, S., Chinnaiyan, A. M., Welling, T. H., Marquez, V. E., Kotarski, J., Wang, H., Wang, Z., Zhang, Y., Liu, R., Wang, G., & Zou, W. (2016). Cancer mediates effector T cell dysfunction by targeting microRNAs and EZH2 via glycolysis restriction. Nature Immunology, 17(1), 95–103. https://doi.org/10.1038/ni.3313